Reactions of Dimethyl Ether with Atomic Oxygen: A Matrix Isolation and a Quantum Chemical Study

Roman Wrobel,[†] Wolfram Sander,*[,†] Elfi Kraka,[‡] and Dieter Cremer*[,‡]

Lehrstuhl für Organische Chemie II der Ruhr-Universität, D-44780 Bochum, Germany, and Theoretical Chemistry, University of Göteborg, Reutersgatan 2, S-41320 Göteborg, Sweden

Received: December 4, 1998; In Final Form: March 8, 1999

The reaction of dimethyl ether (**1**) with atomic oxygen generated by photolysis of ozone or N_2O was examined in low-temperature matrices. The major reaction products are two conformers of methoxymethanol (**5**). IR absorptions of the products were assigned by isotopic labeling (^{18}O and D) and DFT calculations at the B3LYP/6-311++G(d,p) level of theory. The mechanism of the formation of **5**, in particular H abstraction from **1** by atomic oxygen ($O(^3P)$ and $O(^1D)$), was investigated using UMP, UCCSD(T), and UDFT. In both the H abstraction and the $O(^1D)$ insertion reaction, the out-of-plane C−H bonds of **1** are preferentially attacked since the in-plane C−H bonds are about 10 kcal/mol stronger. In the case of a reaction with $O(^3P)$, an Arrhenius activation energy of 3.5 kcal/mol is calculated at 298 K, which compares well with an experimental value of 2.85 kcal/mol. In the exit channel of the reaction, a radical−radical complex between $CH_3CH_2\bullet$ and $\bullet OH$ (−2.7 kcal/mol relative to separated products) is found. The latter is the starting point for the formation of **5** and helps to rationalize the stereoselectivity of the reaction leading to particular conformations of **5**.

Introduction

Dimethyl ether (**1**) and its derivatives have been recently proposed as a diesel fuel substitute.[1,2] Several properties such as high cetane number, reduction of CO and NO_x emissions, and low-cost one-step synthesis from C_1 feedstocks make **1** an attractive diesel fuel. Since the emission of ether **1** to the atmosphere might be harmful to the environment, the atmospheric chemistry of **1** has been recently studied by several authors.[3−6] The oxidation of **1** in the troposphere is mainly initiated by the reaction with hydroxyl radicals leading to the methoxymethyl radical.

$$CH_3OCH_3 + OH \rightarrow CH_3OCH_2 + H_2O$$

The rate of this reaction dictates the atmospheric lifetime of dimethyl ether **1** and influences its greenhouse warming and ozone depletion potential. Once produced, the CH_3OCH_2 radical can participate in further degradation in the atmosphere. The reaction of the CH_3OCH_2 radical with O_2 produces organic peroxy radicals CH_3OCH_2OO, which eventually decompose to formaldehyde.[6−7]

$$CH_3OCH_2 + O_2 \rightarrow CH_3OCH_2OO^{\#}$$

$$CH_3OCH_2OO^{\#} \rightarrow CH_2OCH_2OOH^{\#} \rightarrow 2HCHO + OH$$

Moreover, the radicals are able to react with atmospheric NO_x. The above reaction is the key process to understand the generation of secondary pollutants, such as ozone, various carbonyl compounds and organic nitrogen compounds.[5]

In the laboratory, the CH_3OCH_2 radical can be produced by hydrogen abstraction from dimethyl ether **1** with atomic oxygen. The kinetics of this reaction was investigated by H. LeFevre et al.[8] Alternatively, oxygen atoms might add to **1** and thus provide a simple entry to the $C_2H_6O_2$ potential energy surface. Schwarz and co-workers calculated several stationary points of this potential energy surface at the B3LYP/6-311++G (d,p) level of theory.[9] According to these calculations, the elusive dimethyl ether O-oxide **2** should be 51 kcal/mol higher in energy than dimethylperoxide **4**, however, separated from **4** by a large activation barrier of 34.9 kcal/mol. The exothermic fragmentation of **2** to CH_3OCH_2 and OH radicals is predicted to take place with a barrier of only 25.9 kcal/mol, considerably less than the rearrangement to peroxide **4**, and thus the radical path is the expected major decomposition route. According to the DFT calculations, the reaction of singlet oxygen atoms $O(^1D)$ and **1** to yield ether oxide **2** is exothermic by 44.5 kcal/mol, while triplet oxygen atoms $O(^3P)$ are predicted to produce a weakly bound (2.8 kcal) charge transfer complex **3**.[9]

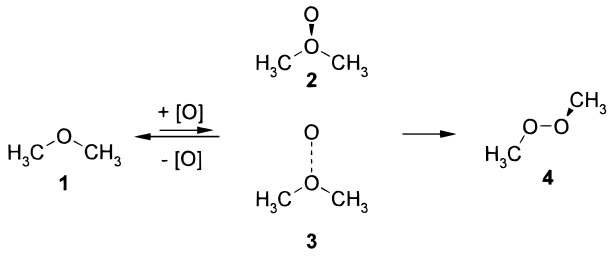

1 **2** **3** **4**

In a similar study, Schriver-Mazzuoli et al.[10] reported on the reaction of CH_4 and CH_3OH with oxygen atoms. These authors found that triplet oxygen atoms $O(^3P)$ are unreactive, while singlet oxygen atoms $O(^1D)$ directly inserted into CH bonds to give CH_3OH and $HOCH_2OH$, respectively. A minor route in the oxidation of CH_3OH was the formation of CH_2O and H_2O. Peroxides or other products with O−O bonds were not observed in this study.

In this work, we investigated the reaction of several isotopomers of dimethyl ether **1** with oxygen atoms under the

[†] Ruhr-Universität Bochum.
[‡] University of Göteborg.

10.1021/jp984631f CCC: $18.00
Published on Web 04/24/1999

conditions of matrix isolation to elucidate the reaction mechanism and to distinguish between the alternatives (i) O-insertion, (ii) O-addition, and (iii) H-abstraction/OH-addition. Our experimental investigation was supported by appropriate ab initio and density functional theory (DFT) calculations.

Results and Discussion

Matrix Isolation Studies. Dimethyl ether **1** and two of its isotopomers (^{18}O-**1** and d_6-**1**) were isolated in an argon matrix at 10 K, and the IR spectra were assigned by comparison with calculations at the B3LYP/6-311++G(d,p) level of theory (Table 1). This assignment is in reasonable agreement with an earlier study on crystalline films of **1**.[11] The most characteristic absorptions of **1** are the asymmetrical COC stretching vibration (ν_{as} COC, #8) at 1173 cm^{-1} and the symmetrical COC stretching vibration (ν_s COC, #4) at 924 cm^{-1}. As expected, ν_{as} COC exhibits a large ^{18}O isotopic shift of 0.981 and a comparatively small deuterium isotopic shift of 0.982. For ν_s COC, the ^{18}O isotopic shift is smaller (0.987), while now a substantial deuterium isotopic shift is observed (0.890). These spectroscopic data are nicely reproduced by the DFT calculations (Table 1).

O(^{1}D) is readily prepared by $\lambda = 266$ nm photolysis of matrix-isolated O_3 (more than 90% yield of O(^{1}D)),[12a] or by $\lambda < 200$ nm photolysis of N_2O.[13,14] In solid argon the lifetime of O(^{1}D) is long enough to escape from the primary matrix cage. Intersystem crossing (ISC) finally produces the ground-state O(^{3}P) which is trapped in interstitial matrix sites.[15] Triplet oxygen atoms can be directly produced by irradiation of O_3 in the near UV or visible region ($\lambda > 360$ nm) of the spectrum.[12b]

Dimethyl ether **1** was matrix-isolated in argon doped with 0.5−5% O_3 at 10 K and irradiated with $\lambda > 420$ nm (Hg arc lamp with cutoff filter) or $\lambda = 248$ nm (KrF Excimer Laser). At high concentrations of O_3 (>1%), the irradiation resulted in a significant broadening of all IR absorptions, presumably due to the formation of complexes of **1** with O_3.[16,17] With 0.5% O_3, narrow line widths were observed, and therefore this concentration was used throughout the experiments described below. However, since under these conditions only a small fraction of **1** is trapped in matrix sites in proximity to O_3 molecules and since the diffusion of trapped species at 8 K is slow, the yield of photooxidation products is low (<5%). On the other hand, the narrow IR line widths allow the spectra to be assigned accurately and experimental and calculated data to be compared.

Irradiation ($\lambda = 248$ nm) of the matrix until complete disappearance of O_3 resulted in the formation of several new IR absorptions (Figure 1), which were stable toward prolonged irradiation. The same set of absorptions was observed when N_2O was used as a source of oxygen atoms, which indicates that O_3 and O_2 are not directly involved in this oxidation process. Since the photolysis of N_2O requires short-wavelength UV irradiation ($\lambda = 193$ nm) and the resulting IR spectra were less well resolved, O_3 was used as the superior source of oxygen atoms in most of the experiments.

By comparison of the new absorptions with the vibrational spectrum of dimethylperoxide **4** reported by Christe,[18] this compound was definitely excluded as a product of the photooxidation. Traces of methanol and formaldehyde were identified by comparison with authentic matrix-isolated material, while the major IR absorptions could not be assigned to known compounds. In the UV/vis spectrum, a new, broad absorption with a maximum at 300 nm was assigned to the oxidation products. A similar absorption was reported by S. Langer et al. for the UV spectrum of the CH_3OCH_2 radical.[5] However, the corresponding IR absorptions assigned to this radical were not observed in our experiments.

TABLE 1: IR Absorptions of Dimethyl Ether 1 Matrix Isolated in Argon at 10 K and B3LYP/6-311++G(d,p) Vibrational Frequencies of 1, Unscaled

		B3LYP/6-311+G(d,p)				argon, 10 K					
no.	sym	CH_3-O-CH_3 ν, [cm^{-1}] (I_{rel})[a]	$CH_3-^{18}O-CH_3$ ν, [cm^{-1}] (I_{rel})[a]	[ν_i/ν]	CD_3-O-CD_3 ν, [cm^{-1}] (I_{rel})[a]	[ν_i/ν]	CH_3-O-CH_3 ν, [cm^{-1}] (I_{rel})[a]	$CH_3-^{18}O-CH_3$ ν, [cm^{-1}] (I_{rel})[a]	[ν_i/ν]	CD_3-O-CD_3 ν, [cm^{-1}] (I_{rel})[a]	[ν_i/ν]	assgnt
1	a_2	203 (0)	203 (0)	1.0	145 (0)	0.714						t CH_3
2	b_1	237 (4)	234 (4)	0.987	184 (4)	0.776						t CH_3
3	a_1	408 (1)	402 (1)	0.985	344 (1)	0.843						δ COC
4	a_1	936 (29)	921 (28)	0.984	831 (15)	0.889	924 (35)	912 (55)	0.987	823 (5)	0.890	ν_s COC + r CH_3
5	b_2	1114 (31)	1100 (51)	0.987	865 (0)	0.776	1096 (45)	1084 (97)	0.989			ν COC + r CH_3
6	a_2	1155 (0)	1155 (0)	1.0	877 (0)	0.759						
7	b_1	1186 (4)	1180 (4)	0.995	937 (6)	0.794				928 (4)		r CH_3
8	b_2	1192 (69)	1169 (42)	0.981	1170 (100)	0.981	1173 (100)	1151 (100)	0.981	1153 (100)	0.982	ν COC + r CH_3
9	a_1	1261 (3)	1251 (2)	0.992	1086 (0)	0.861	1241 (6)	1236 (6)	0.996			δ_s CH_3
10	b_2	1458 (1)	1456 (2)	0.999	1077 (1)	0.739	1425 (1)	1425 (5)	1.0			δ_s CH_3
11	a_2	1478 (0)	1478 (0)	1.0	1068 (0)	0.723						
12	a_1	1484 (0)	1484 (0)	1.0	1059 (10)	0.714				1051 (5)		δ_{as} CH_3
13	b_1	1487 (10)	1487 (10)	1.0	1075 (3)	0.723	1456 (29)	1456 (34)	1.0	1061 (3)	0.729	δ_{as} CH_3
14	b_2	1494 (10)	1494 (9)	1.0	1079 (2)	0.722	1461 (15)	1461 (39)	1.0	1059 (4)	0.724	δ_{as} CH_3
15	a_1	1513 (1)	1512 (1)	0.999	1163 (4)	0.769	1478 (16)	1478 (16)	1.0			δ_{as} CH_3
16	b_2	2958 (41)	2958 (41)	1.0	2121 (33)	0.717	2820 (50)	2820 (98)	1.0	2055 (14)	0.728	ν_s CH_2 + ν CH
17	a_1	2970 (52)	2970 (52)	1.0	2133 (27)	0.718	2869 (15)	2869 (27)	1.0			ν_s CH_2 + ν CH
18	b_1	3003 (100)	3003 (100)	1.0	2226 (59)	0.741	2891 (43)	2891 (95)	1.0	2190 (16)	0.757	ν_{as} CH_2
19	a_2	3008 (0)	3008 (0)	1.0	2232 (0)	0.742	2934 (13)	2934 (48)	1.0			1478 + 1456
20	b_2	3113 (22)	3113 (22)	1.0	2303 (8)	0.740	2939 (19)	2939 (43)	1.0	2250 (5)	0.765	ν CH + ν_s CH_2
21	a_1	3114 (14)	3114 (14)	1.0	2307 (13)	0.741	2986 (24)	2986 (54)	1.0	2310 (1)	0.774	ν CH + ν_s CH_2

[a] Relative intensity based on the strongest absorption.

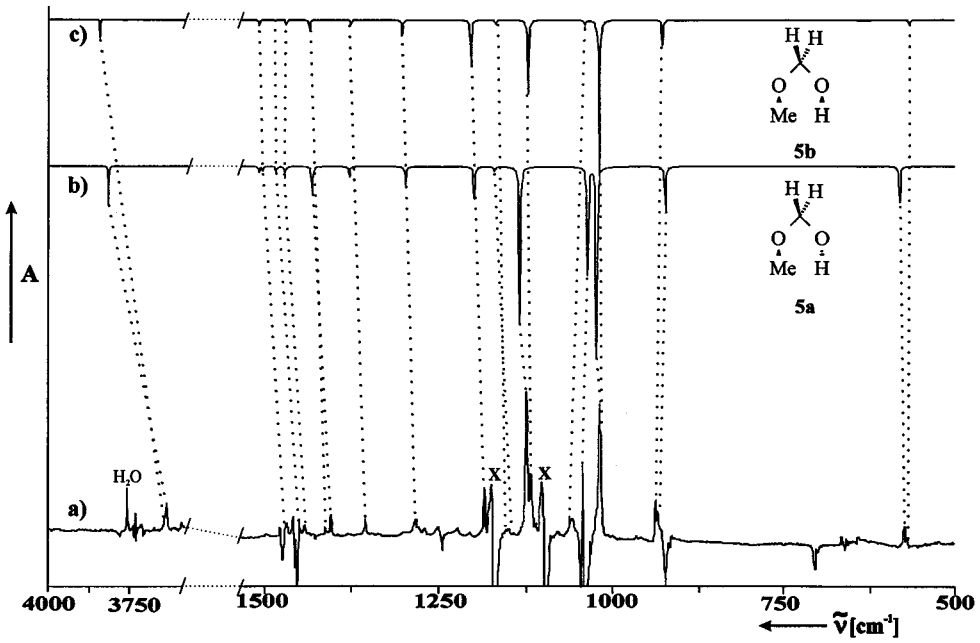

Figure 1. (a) IR difference spectrum showing the oxidation of **1** with atomic O in argon at 10 K after irradiation of the matrix of **1** and ozone (0.8%) with $\lambda = 248$ nm; bottom part, bands disappearing; bands of **5a** and **5b** appearing on irradiation. (b) Calculated spectrum of **5a** at the B3LYP/6311++G(d,p) level of theory, unscaled. (c) Calculated spectrum of **5b** at the B3LYP/6311++G(d,p) level of theory, unscaled.

The IR spectrum of the products obtained by 248 nm irradiation of the **1**/O_3 mixture clearly shows OH stretching vibrations at 3631 and 3641 cm^{-1}, which on deuteration are red-shifted by more than 900 cm^{-1} (Tables 2 and 3). By comparing the IR spectrum with data calculated at the B3LYP/6-311++G(d,p) level of theory, two conformers of methoxymethanol[5] were identified as the main products of the oxidation (Tables 4 and 5). The hemi-acetal[5] is the main product of the equilibrium reaction between formaldehyde and methanol.[19] In substance, **5** is not stable and IR spectra were unknown, so far, while ^1H NMR spectra of **5** could be recorded at low temperature. Since under the conditions of matrix isolation the cleavage of **5** is excluded, alternative mechanisms have to be considered to rationalize the formation of traces of methanol and formaldehyde in our experiments. One route could be the photochemical cleavage of the CO bond of **5** into the CH_3O and CH_2OH radicals. The CH_3O radical rearranges rapidly into the more stable CH_2OH radical,[20−23] which subsequently disproportionates into CH_2O and CH_3OH.[24]

By oxidizing **1**, ^{18}O-**1**, and d_6-**1** with both $^{16}O_3$ and $^{18}O_3$, six isotopomers of **5** were obtained, which allowed a reliable assignment of the IR absorptions. The most characteristic IR absorptions of **5a** are the weak absorption of the combination vibration (ν COC + δ OH, #5) at 576 cm^{-1}, the COC stretching vibration (ν_s COC, #6) at 936 cm^{-1}, the strong absorption at 1020 cm^{-1} (ν COH, #7), a combination vibration (ν COC + CH_2 scis, #8) at 1044 cm^{-1}, and the strongest absorption (ν COC + ω CH2, #9) at 1125 cm^{-1}. Vibration #5 shows a large ^{18}O isotopic shift and a relatively small deuterium isotopic shift (0.925). The symmetrical COC stretching vibration (#6) is blue-shifted compared to the corresponding vibration in **1** and shows similar isotopic ^{18}O or deuterium isotopic shifts. Vibration #7 exhibits both large ^{18}O (0.982) and deuterium (0.959) isotopic shifts on isotopic substitution of the OH group. Vibration #8 is located in the same area as a strong absorption of O_3 and thus not observed in the ^{16}O experiments, but by reaction with $^{18}O_3$ this absorption is clearly observed. #9 shows a large ^{18}O isotopic shift for the isotopic labeling of oxygen by ether **1** (0.981). The CH_2 wag vibration (#14) shows a very large deuterium isotopic shift (0.788) and is the most intense absorption in the perdeuterated **5a**.

The second conformer **5b** is calculated to be higher in energy by 2.1 kcal/mol. The characteristic absorptions are the symmetrical COC stretching vibration (ν_s COC, #6) at 940 cm^{-1}, the very strong combination vibration at 1019 cm^{-1} (ν COH, #7), and the combination vibration at 1119 cm^{-1} (ν COC + ω CH2, #9, Table 3). Isotopic labeling at the OH group results in the expected large ^{18}O (0.985) and deuterium (0.888) isotopic shift of vibration #6. For the strongest absorption, #7, labeling of the OH group leads to a small ^{18}O (0.980) and a relatively large deuterium isotopic shift (0.964). The combination vibration #9 shows a very large ^{18}O isotopic shift on labeling of the ether oxygen atom (0.974). As in **5a**, the most intense absorption after complete deuterium labeling of **5b** with a very large isotopic shift (0.784) is assigned to the CH_2 wag vibration (#14). The position of the OH stretching vibrations (#24) is similar for both conformers of **5** (3631 and 3641 cm^{-1} for **5a** and **5b**, respectively). Both vibrations show a small (0.997) ^{18}O and a very large (0.738) deuterium isotopic shift.

Conformational Behavior of CH_3OCH_2OH (5). There are five forms of **5** in which all vicinal bonds at the CO bonds are staggered: **5-1** (ap,ap), **5-2** (ap,+sc), **5-3** (+sc,ap), **5-4** (+sc,+sc), **5-5** (+sc,−sc) (Scheme 1). Geometry optimizations at the B3LYP/6-311++G(d,p) level of theory show that only three of these forms are close to stable conformers (**5-4** → **5a**, **5-5** → **5b**, **5-2** → **5e**) while forms **5-1** (ap,ap) and **5-3** (+sc,ap) are equal or close to transition states (TS) on the conformational energy surface (CSE) spanned by the two rotational angles τ_1 = ∠MeO−CO and τ_2 = ∠HO−CO of **5** (Scheme 1). Conformation **5a** occupies the global minimum of the CES at τ_1 = 68.9° and τ_2 = 64.9° while **5b** (2.1 kcal/mol relative to **5a**; τ_1 = 69.9°, τ_2 = −85.1°, Scheme 1a) and **5e** (2.2 kcal/mol; τ_1 = 180°, τ_2 = 56.4°, Scheme 1a) correspond to local minima. In a previous investigation of the CES of **5**, Jeffrey, Pople, and Radom found conformational minima similar to **5a** and **5e** but missed **5b** since their work was based on RHF/4-31G theory

TABLE 2: IR Absorptions of Methoxymethanol (5a) Isolated in Argon at 10 K

No.	CH_3-O-CH_2OH ν, [cm^{-1}] (I_{rel})[a]	$CH_3-O-CH_2O^{18}H$ ν, [cm^{-1}] (I_{rel})[a]	[ν_i/ν]	$CH_3-O^{18}-CH_2OH$ ν, [cm^{-1}] (I_{rel})[a]	[ν_i/ν]	$CH_3-O^{18}-CH_2O^{18}H$ ν, [cm^{-1}] (I_{rel})[a]	[ν_i/ν]	CD_3-O-CD_2OD ν, [cm^{-1}] (I_{rel})[a]	[ν_i/ν]	$CD_3-O-CD_2O^{18}D$ ν, [cm^{-1}] (I_{rel})[a]	[ν_i/ν]	assgnt
5	576 (14)	566 (7)	0.983	562 (8)	0.976	554 (8)	0.962	533 (12)	0.925	525 (6)	0.909	ν COC + δ OH
6	936 (20)	936 (31)	1.0	922 (32)	0.985	921 (26)	0.984	833 (28)	0.900	833 (23)	0.900	ν_s COC
7	1020 (94)	1002 (100)	0.982	1119 (80)	0.999	1001 (100)	0.981	978 (25)	0.959	958 (43)	0.939	ν COH
8	1044 (−)	1039 (47)	0.995			1033 (56)	0.990			809 (5)	0.774	ν COC + scisCH_2
9	1125 (100)	1123 (36)	0.998	1104 (44)	0.981	1103 (24)	0.986					ν COC + ω CH_2
10	1150 (2)											-
11	1187 (34)	1185 (24)	0.999	1177 (20)	0.992	1177 (12)	0.992					ω CH_3 + ω CH_2
12	1286 (9)	1285 (7)	0.999	1280 (6)	0.995	1279 (5)	0.995			1027 (8)	0.798	ω CH_3 + ω CH_2
13	1355 (10)	1350 (9)	0.996	1354 (8)	0.999	1348 (8)	0.995	1080 (4)	0.797	1078 (6)	0.795	δ CH_2
14	1406 (3)	1406 (8)	1.0	1402 (11)	0.997	1401 (9)	0.998	1109 (100)	0.788	1108 (100)	0.787	wag CH_2
15	1444 (4)	1443 (4)	0.999	1444 (4)	1.0	1444 (4)	1.0					δ CH_3
16	1452 (7)	1452 (5)	1.0	1452 (5)	1.0	1451 (5)	1.0					
17	1470 (6)	1470 (5)	1.0	1470 (5)	1.0	1470 (6)	1.0					
18								1142 (18)		1131 (18)		δ CH_3
19	2878 (13)	2878 (13)	1.0	2878 (13)	1.0	2878 (13)	1.0	2062 (22)	0.716	2062 (22)	0.716	ν_{as} CH_2
20	2929 (15)	2929 (15)	1.0	2929 (15)	1.0	2929 (15)	1.0					ν_{as} CH_2
21	2964 (13)	2964 (13)	1.0	2964 (13)	1.0	2964 (13)	1.0	2260 (19)	0.762	2260 (19)	0.762	ν CH + ν_s CH_2
22								2346 (16)		2346 (16)		ν CH + ν_s CH_2
23												
24	3631 (18)	3622 (16)	0.997	3631 (19)	1.0	3622 (16)	0.997	2682 (10)	0.737	2664 (10)	0.733	ν O−H

[a] Relative intensity based on the strongest absorption.

TABLE 3: IR-Absorptions of Methoxymethanol (5b) Isolated in Argon at 10 K

No.	CH_3-O-CH_2OH ν, [cm^{-1}] (I_{rel})[a]	$CH_3-O-CH_2O^{18}H$ ν, [cm^{-1}] (I_{rel})[a]	[ν_i/ν]	$CH_3-O^{18}-CH_2OH$ ν, [cm^{-1}] (I_{rel})[a]	[ν_i/ν]	$CH_3-O^{18}-CH_2O^{18}H$ ν, [cm^{-1}] (I_{rel})[a]	[ν_i/ν]	CD_3-O-CD_2OD ν, [cm^{-1}] (I_{rel})[a]	[ν_i/ν]	$CD_3-O-CD_2O^{18}D$ ν, [cm^{-1}] (I_{rel})[a]	[ν_i/ν]	assgnt
5	571 (6)	564 (8)	0.988	558 (8)	0.977	550 (4)	0.963					ν COC + δ OH
6	940 (37)	940 (43)	1.0	926 (38)	0.985	926 (26)	0.985	835 (31)	0.888	835 (45)	0.888	ν_s COC
7	1019 (100)	999 (100)	0.980	1018 (100)	0.998	998 (100)	0.979	982 (25)	0.964	959 (33)	0.941	ν COH
8	1064 (17)											ν COC +scisCH_2
9	1119 (55)	1119 (53)	1.0	1090 (86)	0.974	1090 (79)	0.974					ν COC + ω CH_2
10	1143 (2)											
11	1186 (43)	1185 (24)	0.999	1177 (20)	0.992	1177 (13)	0.992					ω CH_3 + ω CH_2
12	1285 (12)	1280 (6)	0.996	1280 (7)	0.996	1277 (4)	0.994					ω CH_3 + ω CH_2
13	1356 (15)	1350 (7)	0.996	1355 (8)	0.999	1346 (5)	0.993					δ CH_2
14	1414 (5)	1414 (8)	1.0	1412 (2)	0.998	1411 (3)	0.997	1109 (100)	0.784	1109 (100)	0.784	wag CH_2
15	1444 (6)	1444 (4)	1.0	1444 (6)	1.0	1444 (4)	1.0					δ CH_3
16	1452 (6)	1452 (5)	1.0	1452 (6)	1.0	1452 (5)	1.0					δ CH_3
17	1470 (10)	1470 (5)	1.0	1470 (10)	1.0	1470 (5)	1.0					δ CH_3
18								1131 (25)		1131 (25)		δ CH_3
19	2824 (14)	2824 (14)	1.0	2824 (14)	1.0	2824 (14)	1.0	2068 (22)	0.732	2068 (22)	0.732	ν_{as} CH_2
20								2189 (34)		2189 (34)		ν_{as} CH_2
21	2946 (12)	2946 (12)	1.0	2946 (12)	1.0	2946 (12)	1.0	2305 (11)	0.782	2305 (11)	0.782	ν CH + ν_s CH_2
22	3006 (14)	3006 (14)	1.0	3006 (14)	1.0	3006 (14)	1.0					ν CH + ν_s CH_2
23												
24	3641 (11)	3629 (7)	0.997	3641 (11)	1.0	3629 (7)	0.997	2687 (6)	0.738	2670 (5)	0.733	ν O−H

[a] relative intensity based on the strongest absorption.

TABLE 4: Calculated Vibrational Frequencies of Methoxymethanol (5a) at the B3LYP/6-311++G(d,p) Level of Theory, Unscaled

No.	CH_3-O-CH_2OH ν, [cm^{-1}] (I_{rel})[a]	$CH_3-O-CH_2O^{18}H$ ν, [cm^{-1}] (I_{rel})[a]	[ν_i/ν]	$CH_3-O^{18}-CH_2OH$ ν, [cm^{-1}] (I_{rel})[a]	[ν_i/ν]	$CH_3-O^{18}-CH_2O^{18}H$ ν, [cm^{-1}] (I_{rel})[a]	[ν_i/ν]	CD_3-O-CD_2OD ν, [cm^{-1}] (I_{rel})[a]	[ν_i/ν]	$CD_3-O-CD_2O^{18}D$ ν, [cm^{-1}] (I_{rel})[a]	[ν_i/ν]	assgnt
1	144 (2)	143 (2)	0.993	143 (2)	0.993	142 (2)	0.986	107 (0)	0.743	107 (0)	0.743	t CH
2	191 (4)	189 (3)	0.990	190 (5)	0.995	188 (3)	0.984	162 (3)	0.835	160 (3)	0.838	t CH_3
3	358 (44)	356 (35)	0.994	355 (42)	0.992	353 (32)	0.986	275 (35)	0.768	273 (36)	0.763	t OH
4	394 (36)	393 (31)	0.997	390 (42)	0.990	389 (33)	0.987	325 (3)	0.825	324 (4)	0.822	
5	583 (18)	573 (14)	0.983	571 (20)	0.979	561 (14)	0.962	536 (11)	0.919	527 (10)	0.904	ν COC + δ OH
6	925 (23)	925 (18)	1.0	913 (24)	0.987	912 (17)	0.986	834 (13)	0.902	834 (13)	0.902	ν_s COC
7	1024 (100)	1002 (100)	0.978	1024 (81)	1.0	1002 (100)	0.978	979 (43)	0.956	956 (44)	0.934	ν COH
8	1037 (56)	1035 (23)	0.998	1031 (100)	0.994	1029 (34)	0.992	789 (7)	0.761	786 (9)	0.758	νCOC + scis CH_2
9	1134 (81)	1133 (70)	0.999	1112 (75)	0.981	1110 (63)	0.979	1069 (1)	0.945	1068 (1)	0.942	νCOC + ω CH_2
10	1171 (2)	1171 (2)	1.0	1168 (1)	0.997	1168 (1)	0.997	884 (3)	0.755	883 (4)	0.754	ω CH_2
11	1200 (16)	1200 (14)	1.0	1192 (7)	0.993	1192 (5)	0.993	915 (1)	0.763	915 (1)	0.763	ω CH_3 + ω CH_2
12	1299 (9)	1298 (7)	0.999	1292 (9)	0.995	1291 (7)	0.994	1025 (3)	0.798	1022 (3)	0.787	ω CH_3 + ω CH_2
13	1379 (5)	1373 (4)	0.996	1378 (5)	0.999	1372 (4)	0.995	1094 (10)	0.793	1090 (10)	0.790	ω CH_3 + δ CH_2
14	1433 (13)	1432 (11)	0.999	1431 (15)	0.999	1430 (12)	0.998	1113 (100)	0.746	1112 (100)	0.745	wag CH_3
15	1473 (6)	1473 (4)	1.0	1473 (6)	1.0	1473 (4)	1.0	1157 (23)	0.785	1156 (22)	0.785	δ CH_3
16	1486 (2)	1486 (2)	1.0	1485 (3)	1.0	1485 (2)	1.0	1073 (1)	0.722	1073 (1)	0.722	δ CH_3
17	1506 (2)	1506 (1)	1.0	1506 (2)	1.0	1506 (1)	1.0	1086 (3)	0.721	1086 (3)	0.721	δ CH_3
18	1511 (3)	1511 ((2)	1.0	1511 (2)	1.0	1511 (2)	1.0	1153 (35)	0.763	1151 (37)	0.763	δ CH_3
19	2994 (31)	2994 (26)	1.0	2994 (33)	1.0	2994 (26)	1.0	2149 (18)	0.717	2149 (18)	0.717	ν_{as} CH_2
20	3017 (39)	3017 (32)	1.0	3017 (41)	1.0	3017 (32)	1.0	2189 (23)	0.725	2189 (24)	0.725	ν_{as} CH_2
21	3064 (20)	3064 (17)	1.0	3064 (22)	1.0	3064 (17)	1.0	2269 (12)	0.741	2269 (13)	0.741	ν CH + ν_s CH_2
22	3073 (25)	3073 (21)	1.0	3073 (27)	1.0	3073 (21)	1.0	2289 (13)	0.745	2289 (14)	0.745	ν CH + ν_s CH_2
23	3125 (12)	3125 (10)	1.0	3125 (13)	1.0	3125 (10)	1.0	2317 (6)	0.741	2317 (7)	0.741	ν CH + ν_s CH_2
24	3815 (20)	3802 (16)	0.997	3815 (21)	1.0	3802 (16)	0.997	2777 (10)	0.728	2759 (10)	0.723	ν O−H

[a] Relative intensity based on the strongest absorption.

TABLE 5: Calculated Vibrational Frequencies of Methoxymethanol (5b) at the B3LYP/6-311++G(d,p) level of Theory, Unscaled

No.	CH_3-O-CH_2OH ν, [cm^{-1}] (I_{rel})[a]	$CH_3-O-CH_2O^{18}H$ ν, [cm^{-1}] (I_{rel})[a]	[υ_i/ν]	$CH_3-O^{18}-CH_2OH$ ν, [cm^{-1}] (I_{rel})[a]	[υ_i/ν]	$CH_3-O^{18}-CH_2O^{18}H$ ν, [cm^{-1}] (I_{rel})[a]	[υ_i/ν]	CD_3-O-CD_2OD ν, [cm^{-1}] (I_{rel})[a]	[υ_i/ν]	$CD_3-O-CD_2O^{18}D$ ν, [cm^{-1}] (I_{rel})[a]	[υ_i/ν]	assgnt
1	136 (3)	134 (3)	0.985	135 (3)	0.992	133 (3)	0.978	111 (2)	0.816	111 (2)	0.816	t CH
2	194 (2)	193 (2)	0.995	193 (2)	0.995	192 (2)	0.990	151 (5)	0.778	149 (5)	0.768	t CH_3
3	303 (32)	303 (33)	1.0	303 (32)	1.0	302 (32)	0.997	223 (26)	0.736	222 (27)	0.732	t OH
4	392 (11)	389 (11)	0.992	387 (12)	0.987	384 (12)	0.979	331 (6)	0.844	329 (6)	0.839	
5	569 (3)	560 (2)	0.984	555 (2)	0.975	546 (2)	0.959	538 (5)	0.945	528 (5)	0.928	ν COC + δ OH
6	929 (15)	928 (14)	0.999	917 (15)	0.987	917 (14)	0.987	838 (20)	0.902	838 (21)	0.902	ν_s COC
7	1020 (100)	1001 (100)	0.981	1018 (100)	0.998	999 (100)	0.979	976 (51)	0.957	954 (54)	0.935	ν COH
8	1041 (5)	1037 (2)	0.996	1040 (6)	0.999	1036 (2)	0.995	770 (9)	0.740	769 (11)	0.739	ν COC + scis CH_2
9	1122 (44)	1121 (47)	0.999	1098 (48)	0.979	1096 (51)	0.977	1072 (0)	0.955	1072 (0)	0.955	ν COC + ω CH_2
10	1169 (2)	1168 (2)	0.999	1164 (1)	0.996	1164 (1)	0.996	886 (1)	0.758	886 (1)	0.758	ω CH_2
11	1205 (27)	1205 (28)	1.0	1194 (16)	0.991	1194 (16)	0.991	913 (4)	0.758	912 (5)	0.757	ω CH_3 + ω CH_2
12	1304 (9)	1303 (9)	0.999	1297 (9)	0.994	1296 (9)	0.994	1021 (6)	0.783	1017 (5)	0.780	ω CH_3 + ω CH_2
13	1377 (3)	1371 (2)	0.996	1377 (3)	1.0	1371 (2)	0.996	1094 (6)	0.794	1091 (0)	0.792	ω CH_3 + δ CH_2
14	1437 (6)	1436 (6)	0.999	1434 (7)	0.998	1433 (7)	0.997	1111 (100)	0.773	1111 (100)	0.773	wag CH_3
15	1471 (2)	1471 (2)	1.0	1471 (2)	1.0	1471 (2)	1.0	1164 (30)	0.791	1163 (29)	0.791	δ CH_3
16	1488 (1)	1488 (1)	1.0	1488 (1)	1.0	1488 (1)	1.0	1076 (7)	0.723	1075 (10)	0.723	δ CH_3
17	1499 (0)	1499 (0)	1.0	1499 (0)	1.0	1499 (0)	1.0	1088 (12)	0.726	1085 (11)	0.724	δ CH_3
18	1511 (3)	1511 (3)	1.0	1511 (3)	1.0	1511 (3)	1.0	1147 (41)	0.759	1146 (45)	0.759	δ CH_3
19	2955 (28)	2955 (29)	1.0	2955 (28)	1.0	2955 (29)	1.0	2134 (20)	0.722	2134 (21)	0.722	ν_{as} CH_2
20	2973 (27)	2973 (27)	1.0	2973 (27)	1.0	2973 (27)	1.0	2157 (34)	0.726	2157 (35)	0.726	ν_{as} CH_2
21	3033 (19)	3033 (19)	1.0	3033 (19)	1.0	3033 (19)	1.0	2247 (17)	0.741	2247 (18)	0.741	ν CH + ν_s CH_2
22	3121 (8)	3121 (8)	1.0	3121 (8)	1.0	3121 (8)	1.0	2310 (6)	0.740	2310 (6)	0.740	ν CH + ν_s CH_2
23	3128 (8)	3128 (9)	1.0	3128 (8)	1.0	3128 (8)	1.0	2318 (11)	0.741	2318 (12)	0.741	ν CH + ν_s CH_2
24	3842 (11)	3830 (11)	0.997	3842 (11)	1.0	3830 (11)	0.997	2798 (10)	0.728	2780 (10)	0.723	ν O−H

[a] Relative intensity based on the strongest absorption.

SCHEME 1[a]

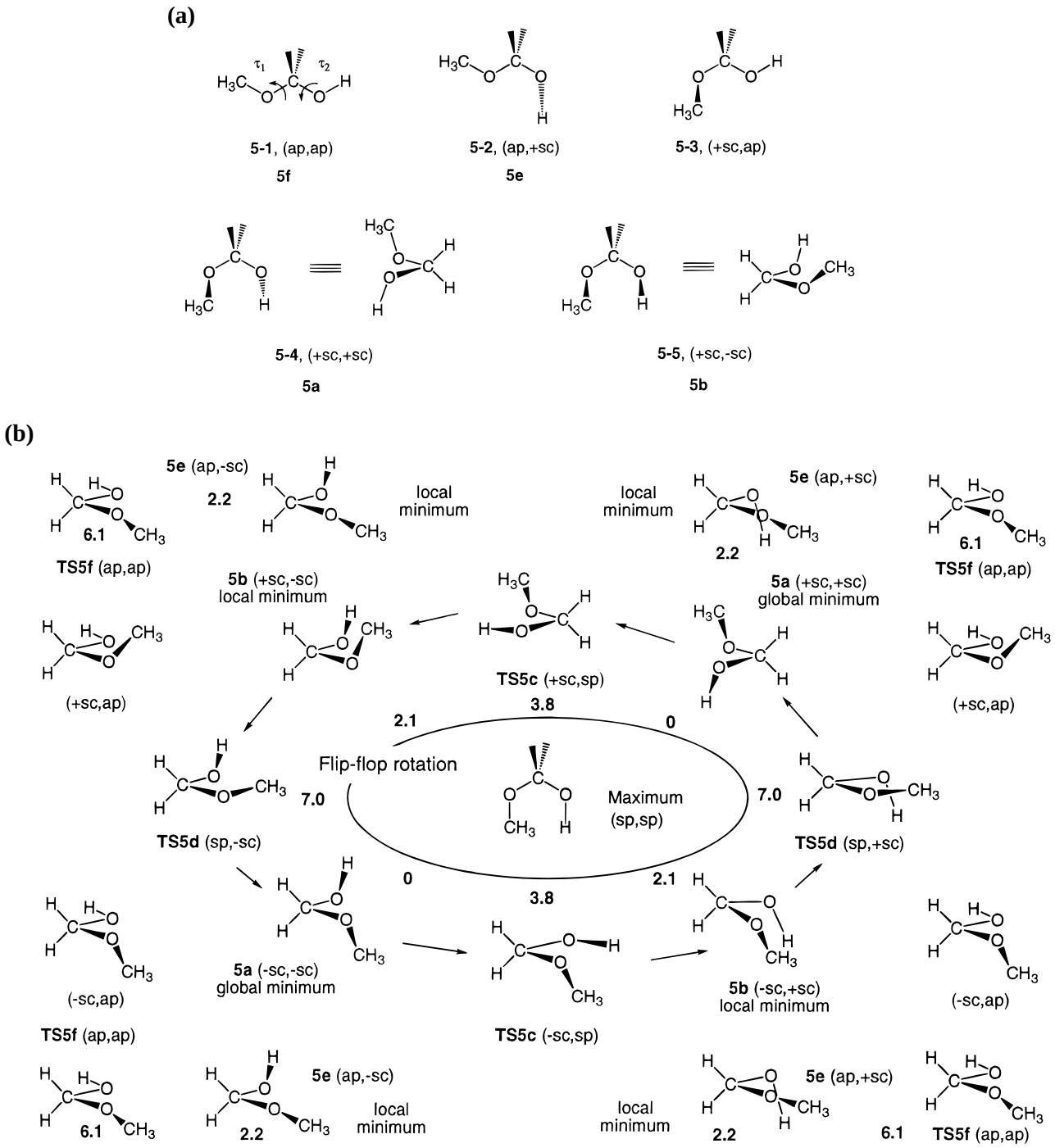

[a] (a) Conformations of **5-1** to **5-5** with perfect staggering at the CO bonds with rotational angles τ_1 and τ_2 indicated. For the (sp,sp) form, $\tau_1 = \tau_2 = 0°$. Lower numbers correspond to stationary points found on the CES of **5**. (b) Flip-flop rotation of **5** (inner circle) as described by the conformers encountered in this process. Relative energies calculated at the B3LYP/6-311++G(d,p) level are also given.

and a rigid rotor model defined by standard geometrical parameters.[25] Such an approach can provide a reasonable account of the topology of the CES; however, the location of stationary points and values of calculated rotational barriers obtained in this way are questionable.

The stability of **5a** and **5b** is caused by anomeric delocalization of one of the electron lone pairs at oxygen into the vicinal CO bond, which will be best accomplished if the OH and OMe bonds are perpendicular to the OCO plane and the electron lone pair orbital and σ^*(CO) orbital strongly overlap.[26] On the other hand, interactions between the OH and OMe bond dipoles determine the energy difference between **5a** (nearly antiparallel arrangement of bond dipoles, attraction) and **5b** (parallel arrangement of bond dipoles, repulsion). The actual values of the dihedral angles OCOR (R = Me and R = H; **5a**, 69° and 65°; **5b**, 70° and −85°; Scheme 1a) are determined by both bond dipole interactions, anomeric delocalization, and second-order hyperconjugation (bond staggering).[27,28]

Conformations **5a** and **5b** are connected by a flip-flop rotation (Scheme 1b) where, contrary to symmetric geminal double rotors such as $X(OY)_2$ (X = CH_2, O, S, etc.; Y = CH_3, OH, SH, etc.[27,28]), the flip-flop potential is characterized by two rather

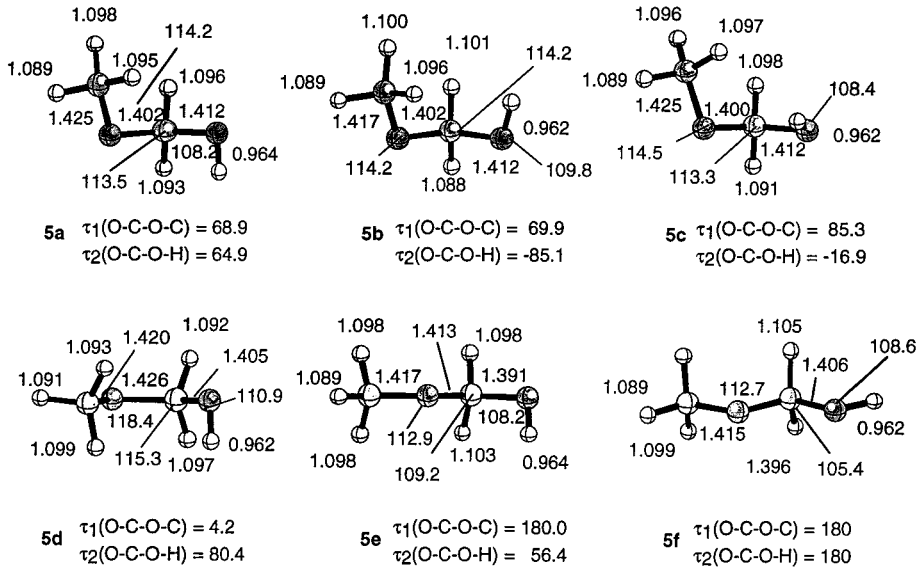

Figure 2. Minimum conformations and rotational transition states of methoxymethanol (**5**) calculated at the B3LYP/6-311++G(d,p) level of theory. Distances in Å, angles in deg. Dihedral angles τ_1 and τ_2 correspond to the convention used in Scheme 1.

than one rotational barrier. Rotation of the OH group (TS-**5c**; $\tau_1 = 85°$, $\tau_2 = -17°$, Scheme 1b and Scheme 1a) is energetically less demanding (rotational barrier: 3.8 kcal/mol) than rotation of the OMe group (TS-**5d** rotational barrier: 7.0 kcal/mol; $\tau_1 = 4°$, $\tau_2 = 80°$; Scheme 1a). As indicated by the two barriers, the anomeric effect of the OMe group is clearly stronger than that of an OH group (reflected also by the two $-H_2C-$OR bond lengths of **5a**: C−OH = 1.412, C−OMe = 1.402 Å; see Figure 2). For comparison, the barriers of rotation in methanol and **1** are 1.1 and 2.7 kcal/mol, respectively.[29]

The flip-flop rotation of a geminal double rotor has been compared with the pseudorotation process of a five-membered ring.[27,28] Accordingly, **5a** corresponds to the twist form of a five-membered ring, while **5b** is related to an envelope form. An "inversion" of **5a** or **5b** is an unlikely conformational process since it would involve simultaneous inward rotation of the two OR groups, thus leading to the sterically strongly hindered (sp,-sp) form, which occupies the global maximum of the conformational energy surface of **5**. Another local minimum of the CES of **5** is associated with the "acyclic" form **5e** (ap,+sc) ($\tau_1 = 180°$, $\tau_2 = 56°$, Scheme 1b and Scheme 1a), while the corresponding (+sc,ap) form is just a transient point on the CES. Form **5e** (2.2 kcal/mol relative to **5a**) benefits from an anomeric interaction of the OH group with the neighboring C−OMe bond and from the anti arrangement with optimal bond staggering of the OMe group. The planar form TS-**5f** (ap,ap; Scheme 1a) is the transition state for the outward directed rotation of the OH-group in **5e** (barrier: 3.9 kcal/mol).

Mechanism of the Formation of 5. The abstraction of an H atom from **1** by O(^{3}P) is slightly exothermic. Utilizing the G2 method,[30] we calculate reaction enthalpies $\Delta\Delta H_f^0(0)$ and $\Delta\Delta H_f^0(298)$ for reaction 1 to be −5.4 and −4.7 kcal/mol, respectively. When these values are combined with the known heats of formation for **1**, O(^{3}P), and the OH radical (0 K, −39.7, 59.0, 9.2; 298 K, −44.0, 59.6, 9.3 kcal/mol[31]), the $\Delta H_f0(0)$ and $\Delta H_f0(298)$ values of radical CH_3OCH_2 (**6**) are calculated to 4.7 and 1.6 kcal/mol, respectively. Various estimates of the heat of formation ranging from −6.9 to −1.3 ± 2 kcal/mol have been published.[32] Good and Francisco[33] have pointed out that these estimates of $\Delta H_f^0(298)$ are probably erroneous due to assumptions made in the experimental work. Their calculated $\Delta H_f^0(0)$ and $\Delta H_f^0(298)$ values of 4.2 and 0.9 kcal/mol, respectively, are in reasonable agreement with our values and suggest that theory is more reliable in this case.[33] The reaction enthalpies for H abstraction by O(^{1}D) are −50.8 (0 K) and −50.1 kcal/mol (298 K), respectively. The latter reaction should proceed without a barrier as is suggested by DFT and MP2 calculations as well as experimental observations.[10] A collinear approach of O(^{1}D) along one of the CH bond axes of **1** does not lead to a stationary point but leads via a bent C···H···O geometry to **5** as soon as linearity constraints are relieved in the geometry optimization. There is a possibility of probing the reactivity of the various CH bonds of **1** with the help of dimethyl ether oxide (modeling O(^{1}D) attack) since H abstraction leads to a finite barrier in this case. It turns out that the out-of-plane H atoms can be more easily attacked than the in-plane H atoms (see below).

$$CH_3OCH_3\ (^1A_1) + O\ (^3P) \rightarrow CH_3OCH_2\ (^2A) + OH\ (^2\Pi) \quad (1)$$

$$CH_3OCH_2\ (^2A) + OH\ (^2\Pi) \rightarrow CH_3OCH_2OH\ (^1A) \quad (2)$$

A computational investigation of H abstraction from **1** by O atoms faces both technical and methodological problems. The reaction mechanism can be complicated by the formation of complexes between **1** and O(^{3}P) or **6** and OH. Little is known about the stability of complexes involving radicals;[34] however, one can assume that the stability of these complexes is determined by the same forces as in the case of normal van der Waals complexes between closed-shell systems. On the other hand, the transition state energy for H abstraction by a radical will be low and, therefore, the potential energy surface (PES) along the path of the H abstraction will be rather flat. This means that the existence of a van der Waals complex as a precursor to the actual reaction complex will depend strongly on secondary effects such as zero-point energies (ZPE) and entropies rather than electronic effects. Therefore, the mechanistic relevance of complex formation in the H abstraction reaction is decided on the enthalpy (ΔH) or free enthalpy (ΔG) hypersurface (PHS or PGS) rather than the PES. There are examples in the literature which show that changes in ZPEs, temperature effects, and entropies rather than electronic changes along the reaction path can determine a reaction mechanism.[35]

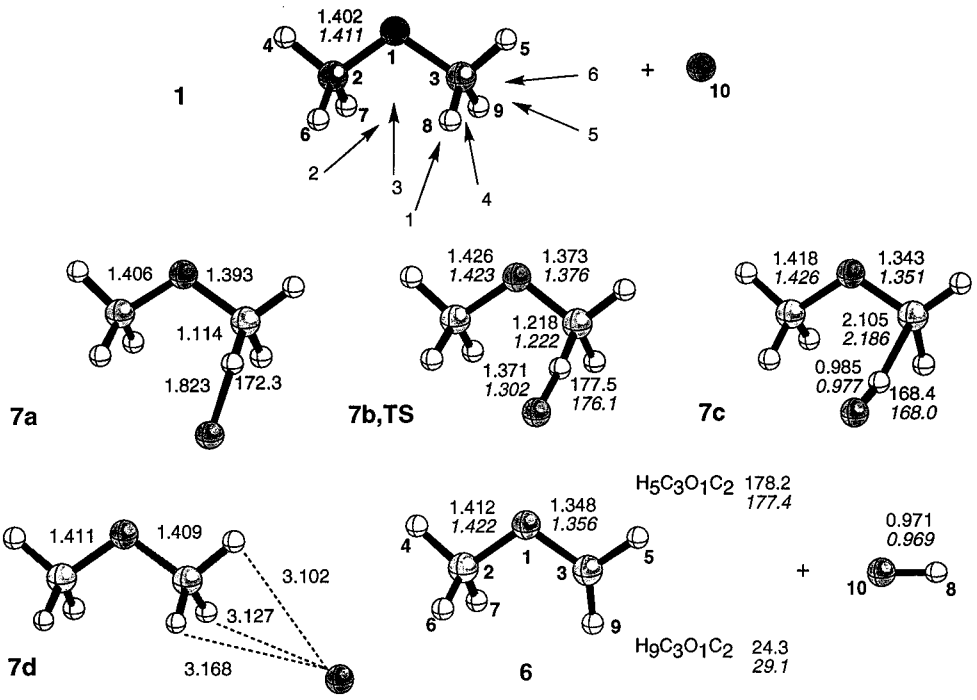

Figure 3. Geometries of dimethyl ether (**1**), CH_3OCH_2• radical (**6**), and stationary points **7** of the collision complexes between **1** and O(3P) calculated at the UMPW1PW91/6-311++G(d,p) (normal print) and UMP2/6-311++G(d,p) level of theory (italics). For **1**, the most likely directions of attack by O(3P) are indicated by arrows.

DFT has been found to seriously fail with regard to the description of radical reactions such as $H + H_2 \rightarrow H_2 + H$,[36] $OH + H_2 \rightarrow HOH + H$,[37] $O(^3P) + CH_4 \rightarrow CH_3 + OH$,[38] etc. This is mainly due to the self-interaction error[39] caused by not using exact exchange in DFT as calculations with appropriate self-interaction correction (SIC) have shown.[36,40] The SIC problem is partially avoided in hybrid DFT methods, which use exact exchange (at least partially). Hence, hybrid DFT methods provide a reasonable description of the energetics of reactions such as $OH + H \rightarrow HOH + H$.[37] Also, B3LYP[41] or the recently developed MPW1PW91 one-parameter hybrid functional[42] are able to describe H-bonded complexes or in general van der Waals complexes better than standard DFT methods, provided a TZP basis with diffuse basis functions is used (see Experimental Section and refs 42 and 43). However, the rule of thumb is that the DFT description of a van der Waals complex is more problematic the more the complex stability is dominated by dispersion rather than electrostatic interactions.[44] Taking this into consideration, we used unrestricted B3LYP and MPW1PW91 to explore the mechanism of reactions 1 and 2 and, then, we analyzed results with the help of UMP2 and UCCSD(T) calculations for the same compounds involved.

If one considers that exchange repulsion, polarization, and dispersion forces should dominate the interactions between $O(^3P)$ and **1**, then complex formation should preferentially be expected in regions 3, 2, 4, 5, 6, 1, and 7 of **1** (see Figure 3), since in this order exchange repulsion will increase while stabilizing dispersion and polarization forces will decrease. Actually, explorative calculations with a DZP basis in these regions surrounding **1** led to the discovery of three complexes, three first-order transition states, and two second-order transition states. Utilizing these stationary points for refined descriptions with the 6-311++G(d,p) basis at UB3LYP and UMPW1PW91 structures **7a** (complex between **1** and $O(^3P)$, **7b** (transition state), **7c** (complex between **6** and •OH), and other structures such as **7d** (complex between **1** and $O(^3P)$, see Figure 3 and Table 7) were found. The corresponding energies, enthalpies, and free enthalpies are given in Table 6.

Clearly, **7a**, **7b**, and **7c** are located at three consecutive stationary points along the path of reaction 1 involving one of the out-of-plane H atoms. A similar approach of $O(^3P)$ in the direction of the bond axis of CH (in-plane) involves a second-order TS, which is about 8 kcal/mol higher in energy than TS **7b**. An adiabatic analysis[45,46] of the B3LYP/6-311++G(d,p) vibrational modes of **1** leads to adiabatic CH stretching frequencies of 3102 cm^{-1} (in plane) and 2980 cm^{-1} (out-of-plane) (force constants, k (in-plane) = 5.271, k (out-of-plane) = 4.864 mdyn/Å; exptl stretching frequencies, 2981, 2874 cm^{-1}), which according to the relationships given by Larsson and Cremer[47] corresponds to CH dissociation energies D_e = 112.4 and 102.3 kcal/mol (D_0 = 103.8 and 93.7 kcal/mol), respectively. This indicates that abstraction of an out-of-plane H atom should be 10 kcal/mol easier than that of an in-plane H atom of **1** in line with the DFT results obtained for the reaction of **1** with $O(^1D)$ or $O(^3P)$. Also, abstraction of an out-of-plane H atom leads to the more stable CH_3OCH_2• form, as can be seen by comparing the geometries of **7a**, **7b**, and **7c** with that of radical **6** (see Figure 3 and Table 7). While these considerations apply to a fictitious molecule **1** at rest, one has to consider that in the real situation the methyl groups of **1** are rapidly rotating. Hence, an attack of an O atom at the in-plane H will lead to CH bond rupture and H transfer if the O atom can follow the movement of the H atom in an out-of-plane position where a rupture of the CH bonds becomes easier.

The PES is rather flat for an approach of $O(^3P)$ toward one of the out-of-plane H atoms. At UB3LYP/6-311++(d,p), complex **7a** is 1.7 kcal/mol (after BSSE corrections; 2.0 kcal/mol after additional ZPE corrections) below the separated reactants, but its stability decreases to 0.1 kcal/mol for the more reliable MPW1PW91 hybrid functional. At the UMP2/6-311++(d,p) level, **7a** no longer exists, which clearly shows that UB3LYP exaggerates stabilizing O,H interactions at short O10, H8 distances (Figure 3 and Table 7) and leads to spurious van der Waals complexes such as **7d**. This tendency decreases when using the MPW1PW91 functional, but nevertheless it is also a

TABLE 6: Energetics of Reaction 1 Calculated at Various Levels of Theory[a]

compd	ΔE	ΔE(BSSE)	ZPE	E_o	ΔH(298)	ΔG(298)	μ	ω
			I. B3LYP/6-31G(d,p)					
1 + O (^{3}P)	−230.09359	0	50.1	0	−230.00608	−230.05335	1.27	221
7a	−2.7	−1.1	50.3	−1.0	−1.2	4.4	0.95	73
7b	−1.4	−0.1	47.2	−3.1	−3.6	3.5	2.17	888i
7c	−9.2	−7.7	48.9	−8.9	−9.0	−3.4	2.18	101
6 + OH·	−2.4	−2.4	46.7	−5.8	−5.2	−7.8	1.35	171
barrier	1.2	1.0	−			−3.5		
stability of **7c**	−6.8	−5.2	−	−3.1	−3.8			
			II. B3LYP/6-311++G(d,p)					
1 + O (^{3}P)	−230.16699	0	49.7	0	−230.08010	−230.12750	1.44	205
7a	−2.0	−1.7	49.3	−2.0	−2.2	3.1	1.65	47
7b	−1.7	−1.4	47.2	−3.8	−4.6	2.3	2.67	442i
7c	−10.8	−10.5	48.1	−12.2	−12.0	−7.5	2.96	37
6 + OH•	−6.2	−6.3	46.3	−9.7	−9.3	−11.7	1.50	159
barrier	0.3	0.3						
stability of **7c**	−4.3	−4.2		−2.5	−2.6			
			III. MPW1PW91/6-311++(d,p)					
1 + O (^{3}P)	−230.0990	0	50.2	0	−230.01142	−230.05878	1.42	207
7a	−0.4	−0.1	45.0	−0.3	−0.3	3.9	1.22	17
7b	0.4	0.7	47.5	−1.9	−2.7	4.3	2.56	547i
7c	−9.4	−9.1	48.5	−10.7	−10.5	−6.1	2.90	37
6 + OH•	−5.0	−5.1	46.8	−8.5	−7.8	−10.1	1.45	163
barrier	0.7	0.8				−4.3		
stability of **7c**	−4.4	−4.0		−2.3	−2.7	−4.0		
			IV. MP2(frozen)/6-311++G(d,p)					
1 + O (^{3}P)	−229.54715	0	50.8	0	−229.45703	−229.50434	1.65	198
7b (barrier)	14.9	15.2	47.6	12.1	10.6	17.2	1.51	2077i
7c	−2.1	−1.7	49.5	−3.0	−3.7	0.0	2.77	41
6 + OH·	0.2	−0.3	47.6	−3.6	−2.8	−5.3	1.56	169
barrier	14.2	15.2		12.1	10.6	17.2		
stability of **7c**	−2.3	−1.3			−0.9			
			V. CCSD(T,frozen)/6-311++G(d,p)//MP2(frozen)/6-311++G(d,p)					
1 + O (^{3}P)	−229.61362	0	50.8	0	−229.52350	−229.57081		
7b (barrier)	10.2	10.6	47.6	7.4	5.9	12.5		
7c	−2.8	−2.4	49.5	−3.7	−4.4	−0.7		
6 + OH•	0.8	0.3	47.6	−2.9	−2.1	−4.6		
barrier (corrected)[b]	7.6−t	8.0−t		4.8-t	2.3	8.9		$E_a = 3.5$
stability of **7c**	−3.6	−2.7		−0.8	−2.3			

[a] Absolute energies of reference system 1 + O(3P) in hartree, relative energies values in kcal/mol. Δ(BSSE), energy differences after basis set superposition corrections; ZPE, zero-pint corrections; E_0, energy differences at 0 K after ZPE corrections; ΔH(298) and ΔG(298), enthalpy and free enthalpy differences at 298 K; μ, dipole moments in Debye; ω, lowest vibrational frequency in cm^{-1}. For UCCSD(T) results, vibrational and temperature corrections were taken from UMP2 calculations. [b] Corrections comprise the G2 correction of −2.6 kcal/mol and the Wigner tunneling correction of −0.96 kcal/mol at 298 K. See text. Tunneling corrections at 8 K can no longer calculated by the Wigner formula, and therefore, the correction due to tunneling is indicated by t. E_a is the calculated Arrhenius activation energy at 298 K.

basic deficiency of the new functional, which was actually designed to improve the description of van der Waals complexes.[42]

As a direct consequence of exaggerating bonding interactions between O10 and H8, the reaction barrier (TS-**7b**) is underestimated by about 6 kcal/mol (see below), where it does not matter whether UB3LYP (0.3 kcal/mol) or UMPW1PW91 (0.8 kcal/mol), a large or a small basis set, is used (Table 6). UMP2 exaggerates at the same time the barrier by about 8 kcal/mol, suggesting a value of 15 kcal/mol. Despite the large difference in calculated energies, both UDFT and UMP2 suggest similar geometries for TS-**7b**. The O10, H8 distance varies between 1.37 Å (UDFT) and 1.30 Å (UMP2), while the C3, H8 distance is predicted to be 1.2 Å by all three methods (Figure 3). Calculated geometries are qualitatively in line with what one can expect for the geometry of TS-**7b**.

While it is presently not possible to improve the description of a TS such as **7b** at the DFT level, more reliable calculations can be employed at the ab initio level. UCCSD(T)/6-311++G(d,p) predicts a barrier of 10.6 kcal/mol at the UMP2 geometry. The corresponding activation enthalpy at 298 K is 5.9 kcal/mol, and the free activation energy is 12.5 kcal/mol. These values have to be corrected since tunneling should play an important role for reaction 1. At 298 K, a Wigner correction[48] of 0.96 kcal/mol is obtained, which leads to a tunneling corrected activation enthalpy $\Delta H^{\#}$ of 4.9 kcal/mol. From G2 calculations, we can estimate that an increase of the basis set and higher order correlation effects will lead to an additional lowering of the barrier by 2.6 kcal/mol, which is similar to the error in the calculated UCCSD(T) heat of reaction at 298 K (−2.1 kcal/mol compared to the G2 value of −4.7 kcal/mol; see Table 6). This is in line with results of previous investigations on the system OH + H_2 → HOH + H, which showed that geometry optimization of a TS such as **7b** at UCCSD(T) with a QZ3P-(2f1g) basis set can lower the barrier by about 2−3 kcal/mol.[49] Hence, the final $\Delta H^{\#}$(298) obtained in this way is 2.3 kcal/mol.

LeFevre and co-workers obtained an Arrhenius activation energy of $E_a = 2.85 \pm 0.5$ kcal/mol by combining mass-spectrometric and ESR results.[8] Since $E_a = \Delta H^{\#} + 2RT$ for reaction 1, the experimental value compares well with the UCCSD(T) estimate of $E_a = 3.5$ kcal/mol. As for the reaction barrier at 8 K (temperature of reaction in the matrix), we obtain a value of 7.4 kcal/mol, which has to be corrected by 2.6−4.8

TABLE 7: Calculated Geometries of Stationary Points Encountered in Reaction 1 (Compare with Figure 3)[a]

method basis parameter	B3LYP A	B3LYP B	MPW1PW91 B	MP2 B	B3LYP A	B3LYP B	MPW1PW91 B	MP2 B
	7a					**7b**		
H8O10	1.950	1.692	1.823	2.867	1.310	1.369	1.371	1.302
O1C2	1.415	1.419	1.406	1.411	1.426	1.426	1.426	1.423
O1C3	1.402	1.391	1.393	1.410	1.372	1.373	1.373	1.376
C3H5	1.094	1.090	1.089	1.091	1.091	1.089	1.089	1.090
C3H8	1.116	1.113	1.114	1.099	1.251	1.218	1.218	1.222
C3H9	1.101	1.098	1.098	1.099	1.100	1.098	1.099	1.098
C3H8O10	154.3	172.8	172.3	174.0	168.0	177.5	177.5	176.1
C2O1C3	112.3	113.6	112.7	110.8	113.6	114.6	114.6	112.1
O1C3H5	108.0	108.5	107.8	107.4	109.8	109.6	109.7	109.8
O1C3H8	111.1	111.0	110.6	111.3	109.6	110.5	110.5	110.3
O1C3H9	112.4	112.7	112.2	111.3	114.5	114.1	114.1	114.0
H8C3H9	107.0	106.1	107.7	108.5	102.4	103.5	103.4	103.7
H5C3O1C2	180.2	176.4	176.1	180.3	177.6	173.8	173.8	179.3
H8C3O1C2	−60.8	−65.5	−65.7	−60.3	−65.4	−70.2	−70.2	−64.9
H9C3O1C2	59.1	53.3	54.6	60.9	49.0	45.9	45.9	51.3
	7c					**6**		
H8O10	0.996	0.990	0.985	0.977				
O1C2	1.431	1.429	1.418	1.426	1.420	1.423	1.412	1.422
O1C3	1.353	1.350	1.343	1.351	1.360	1.354	1.348	1.356
C3H5	1.085	1.089	1.082	1.083	1.083	1.080	1.080	1.081
C3H8	2.072	2.118	2.105	2.186				
C3H9	1.092	1.089	1.088	1.089	1.090	1.087	1.086	1.088
C3H8O10	155.2	168.4	168.4	168.0				
C2O1C3	115.0	115.9	115,4	114.0	114.9	115.4	114.9	113.4
O1C3H5	112.8	113.2	113.4	113.0	113.1	113.9	113.9	113.2
O1C3H8	99.4	101.9	101.8	101.6				
O1C3H9	117.7	118.0	118.0	117.6	118.1	118.6	118.6	117.6
H8C3H9	92.4	96.2	96.3	97.6				
H5C3O1C2	176.2	174.7	175.1	174.3	176.6	177.7	178.2	177.4
H8C3O1C2	−66.5	−77.5	−77.2	−77.6				
H9C3O1C2	31.3	26.3	26.5	27.6	28.4	23.7	24.3	29.1
H5C3H9	120.4	120.3	120.4	120.2	120.4	121.9	121.7	120.6
	1					**OH**		
H8O10					0.980	0.976	0.971	0.969
O1C2	1.411	1.413	1.402	1.411				
C3H5	1.092	1.090	1.090	1.090				
C3H8	1.102	1.100	1.100	1.099				
C2O1C3	112.3	112.7	112.4	110.8				
O1C3H5	107.4	107.3	107.6	107.4				
O1C3H8	111.9	111.5	111.5	111.2				
H8C3H9	108.5	108.5	108.3	109.2				

[a] Basis sets are denoted in short form: A = 6-31G(d,p); B = 6-311++G(d,p). All bond lengths in Å, bond angles in deg. [b] For **7a**, the UMP2 optimization led to a second-order TS with two imaginary frequencies.

kcal/mol. Assuming that the calculated temperature corrections are reasonable, the corresponding experimental value should be 4.2 kcal/mol. At this temperature, tunneling is large (but can no longer be estimated by the Wigner formula[48b]) so that the barrier becomes effectively zero.

In the exit channel of reaction 1, both UDFT, UMP2, and UCCSD(T) predict the existence of a radical−radical complex **7c** formed by **6** and OH in a triplet state. The predicted stability of complex **7c** ranges from 1.3 kcal/mol (UMP2) to maximally 5.2 kcal/mol (Table 6), where again DFT seems to exaggerate stabilizing interactions between the radical partners. Inclusion of ZPE corrections reduces the complex stability to 0.8 (UCCSD(T)) and 2.5 kcal/mol (UB3LYP/6-311++G(d,p)), while the calculated enthalpy differences at 298 K suggest a stable complex also on the PHS (stability: 0.9−3.5 kcal/mol; Table 6) irrespective of the method and basis set used. Entropy destroys the complex as is suggested by calculated $\Delta G(298)$ values (Table 6).

The various geometries calculated for **7c** show the same relatively small variation in dependence of the method and basis set used as was found for TS-**7b** (Figure 3 and Table 7). At UMP2, the OH bond length of the donor molecule OH is lengthened by 0.008 Å similarly as one has found for the H_2O dimer (0.006 Å).[50] Considering that a CH bond (1.09 Å) is about 0.14 Å longer than a OH bond (0.95 Å), the OC distance should be about 3.12 Å if one uses the experimental OO distance (2.98 Å) in the water dimer.[50] The calculated OC distance is 3.15 Å (UMP2) but somewhat smaller when UDFT is applied (3.00−3.08 Å, Table 7), which reflects the exaggeration of stabilizing interactions at DFT. The stability of H-bond complex **7c** (UCCSD(T): 2.7 kcal/mol, Table 6) is about half of that of the water dimer (5 kcal/mol).[50] Clearly, theory suggests the existence of an H bonded triplet complex between OH and **6** where the donor is a radical and the acceptor is a C atom with a single electron. Such complexes should also exist in other reactions involving $O(^3P)$; however, it will be difficult to detect these complexes since the excess energy such a complex will possess (about 5 kcal/mol if one considers a barrier of 2.3 kcal/mol; see above) should be higher than the complex stability.

Despite the somewhat different descriptions provided by UDFT, UCCSD(T), and UMP2, all theories agree with regard to predictions relevant for the experiments carried out at 8 K in this work. The energetically most favorable attack of $O(^3P)$ is at one of the out-of-plane H atoms of **1**, and there is no energy barrier since H tunneling will reduce a barrier of 4.8 kcal/mol effectively to zero.

Recombination of radicals **6** and OH (reaction 2) should occur within a cavity of the matrix at 10 K without a barrier. Formation

SCHEME 2. Recombination of CH_3OCH_2 and OH Radical Assuming the Geometry of Complex 7c[a]

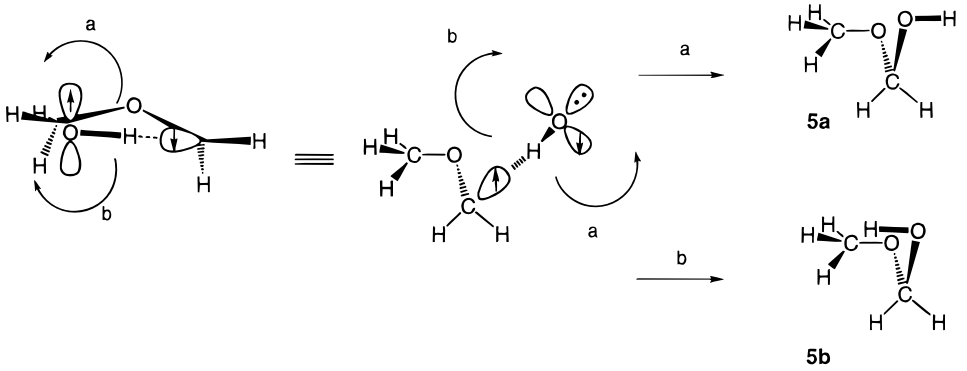

[a] Rotation a is sterically less hindered and leads to **5A**, rotation b to **5b**.

of **5** is strongly exothermic ($\Delta\Delta H_f^0(0)$ and $\Delta\Delta H_f^0(298)$: −98.5, −100.1 kcal/mol, G2 calculations). The heats of formation ΔH_f^0-(O) and $\Delta H_f^0(298)$ of **5** can be calculated from reactions 1 and 2 ($\Delta\Delta H_f^0(0)$ and $\Delta\Delta H_f^0(298)$, −103.9, −104.8 kcal/mol; values for O(^{1}D) insertion into **1** −149.3, −150.2 kcal/mol) to be −84.6 and −89.2 kcal/mol, respectively, which agrees well with an $\Delta H_f^0(298,5)$ estimate of −89.4 based on thermochemical group increments.[51]

It is interesting to note that radical **6** is no longer a pure π-radical. Pyramidalization at the radical center is given by the difference 360 − Σ (C bond angles) = 8.5° (for the geometry, see Figure 3 and Table 7). Clearly, this is a result of destabilizing three-electron interactions involving a single π electron at C and the two electrons occupying a pπ lone pair orbital at O. Theory shows that this can be avoided by (a) reducing the overlap between the orbitals involved and (b) increasing the difference between the corresponding orbital energies. Hence, the σ nature of radical **6** is in line with observations made for $\bullet CH_2X$ (X = OH, F, Cl) radicals.[52]

In TS-**7b** as well as complex **7c**, the equilibrium geometry of radical **6** is largely developed. If the OH group rotates as shown in Scheme 2 where the rotation may be initiated by a large amplitude OHC bending vibration, then, depending on the direction of rotation, conformations **5a** or **5b** will be directly formed. Steric interactions should be smaller for rotation (a) in Scheme 2 (thus leading to more **5a**); however, this depends on the actual distance between **6** and OH, for which rotation will become possible.

Conclusion

The oxidation of dimethyl ether **1** with atomic oxygen generated by photolysis of ozone or N_2O has been examined in low-temperature matrixes. The major reaction products are the two most stable conformers of methoxymethanol, **5a** and **5b**, while the third conformation **5e** was not found among the reaction products. The weakly bound (2.8 kcal) charge transfer complex of dimethyl ether with atomic oxygen O(^{3}P), **3**, was also not observed. Experience collected in this work suggests that such a complex does not exist and is just an artifact of the DFT calculation used in ref 9.

Three mechanisms have to be considered to rationalize the formation of **5**.

(i) The most reasonable mechanism is the hydrogen abstraction from **1** to give **6** and OH radicals, which by in-cage recombination produce **5**. According to a calculated heat of formation of 4.7 kcal/mol (at 0 K), radical **6** is quite stable, however, due to a rapid in-cage reaction not observed in the experiments. This mechanism requires that the small OH radical does not escape the matrix cage in significant amounts.

(ii) The second mechanism is the direct insertion of O(1D) into a CH bond of ether **1** without formation of intermediate radicals.

(iii) The third mechanism **1** is the rearrangement of dimethyl ether O-oxide **2** formed as a short-lived intermediate. The barrier for the fragmentation of **2** into **6** and OH radicals is predicted to be 25.9 kcal/mol, and these radicals could recombine to **5** as described above. However, with an activation barrier of only 16 kcal/mol, the fragmentation into CH_3 and CH_3OO represents the lowest exit channel for **2**.[9] Neither of these radicals nor their recombination product dimethylperoxide **4** could be observed in the IR spectrum. Thus, the route via dimethyl ether O-oxide **2** can clearly be excluded as a possible mechanism for the oxidation of ether **1**.

Possibilities (i) or (ii) are both likely as reaction mechanism. H abstraction by O(^{3}P) occurs preferentially at the out-of-plane CH bonds of **1** and in this case the activation energy of reaction 1 is effectively zero. The calculated Arrhenius energy of 3.5 kcal/mol at 298 is in agreement with an experimental E_a of 2.85 ± 0.5 kcal/mol.

Stabilization of radical **6** by three-electron interactions, which are already active in TS-**7b** lower the barrier by about 2 kcal/mol as can be deduced from the activation enthalpies measured for the corresponding reaction in the case of alkanes (propane + O(^{3}P): 5 kcal/mol).[53]

As an unexpected result of the investigation of the reaction mechanism, we found a H-bonded radical−radical complex in a triplet state that involves C as an acceptor. To the best of our knowledge, such complexes have never been described before and, although their experimental verification may be difficult, they should play an important role in the elucidation of the reaction mechanism involving radicals.

Experimental Section

Matrix Spectroscopy. Matrix isolation experiments were performed by standard techniques with an APD CSW-202 Displex closed cycle helium cryostat. Matrixes were produced by deposition of argon (Messer-Griesheim, 99.9999%), mixtures of argon, dimethyl ether, and ozone, or mixtures of argon, dimethyl ether, and nitrous oxide on top of a CsI (IR) or sapphire (UV−vis) window with a rate of approximately 0.15 mmol/min. To obtain optically clear matrixes, the cold window was retained at 25−30 K (Ar/ether/ozone) or 17 K (Ar/ether/N2O) during deposition and afterward cooled to 7−9 K.

Infrared spectra were recorded by using a Bruker IFS66 FTIR spectrometer with a standard resolution of 1 cm^{-1} in the range

of 400−4000 cm^{-1}. Irradiations were carried out with use of a KrF Excimer Laser ($\lambda = 248$ nm) or ArF Excimer Laser ($\lambda = 193$ nm) (LPX 105 SD Lambda-Physic) or with use of an Osram HBO 500 W/2 mercury high-pressure arc lamp in Oriel housings equipped with quartz optics. IR irradiation from the lamps was absorbed by a 10 cm path of water. Schott cut off filters were used (50% transmission at the wavelength specified) in combination with dichroic mirrors.

Computational Details. Investigations were carried out employing different levels of theory. Restricted and unrestricted Kohn−Sham theory was applied using two different hybrid functionals, namely Becke's three-parameter functional B3LYP[41] and the modified Perdew−Wang functional described in ref 42, which is supposed to describe van der Waals complexes more accurately. Pople's 6-31G(d,p) and 6-311++G(d,p) basis sets[54] were employed to determine geometry, conformation, and vibrational spectra of **1**, **5**, **6**, and **7**, where the VTZ basis with the diffuse functions was needed in particular for the description of molecular complexes formed in reactions 1 and 2. For the investigation of the latter as well as the insertion of $O(^1D)$ into **1**, B3LYP and MPW1PW91 results were checked by employing unrestricted MP2 and MP4 perturbation theory[56] as well as unrestricted CCSD(T) theory where for MP4 and CCSD(T) only single-point calculations were carried out. For the radicals investigated, spin contamination was determined by calculating the expectation value of S^2, which in no case deviated from the ideal values by more than 10%.

For all molecules and transition states considered, vibrational frequencies at optimized geometries were determined to characterize stationary points. Zero-point energy (ZPE) and thermal corrections were used to obtain reaction and activation enthalpies at 298 K. The determination of entropies led to free enthalpies at 298 K. Some of these calculations were carried out for nonstationary points. In these cases, the determination of vibrational corrections was based on generalized vibrational modes.[57] Reaction energies and enthalpies of reactions 1 and 2 were determined with the help of G2 theory according to standard procedures described in the literature.[30] Utilizing experimental heats of formation $\Delta H_f^0(298)$ for suitable reference compounds,[31] heats of formation for radical **6** and closed-shell molecule **5** were determined.

For the van der Waals complexes **7**, basis set superposition errors (BSSE) were corrected with the help of the counterpoise method.[58] Calculations were carried out with COLOGNE96,[59] ACES,[60] GAUSSIAN94,[61] and GAUSSIAN98.[62]

Materials. Mass spectra (EI, 70 eV) were taken on a Varian MAT CH5.

Dimethyl ether **1** was obtained from Aldrich Company (99% purity) and used without further purification. Dimethyl ether-18O was prepared by a procedure described by Blukis, Kasai, and Myers.[63] By mass spectroscopy the ^{18}O content was determined to be 86%. Dimethyl ether-d_6 was prepared by a procedure described by Kanazawa and Nukada,[64] and the deuterium content was determined to be 99%. Ozone and Ozone-^{18}O were generated with an ozonizer (Demag), trapped at 77 K, and purified according to ref 65. Ozone-^{18}O was obtained by using $^{18}O_2$ (99.5% isotopic purity) in the procedure described above. Nitrous oxid N_2O was obtained from Air Liquide Company (99.9% purity).

Acknowledgment. We thank Dr. Ch. Schalley, Dr. D. Schröder, and Prof. Dr. H. Schwarz, Technical University of Berlin, for intensive and stimulating discussions. At the University of Bochum, this work was financially supported by the Deutsche Forschungsgemeinschaft (Schwerpunktprogramm "Peroxidchemie") and the Fonds der Chemischen Industrie. At Göteborg University, financial support was provided by the NFR. Calculations were done on a CRAY C90 of the Nationellt Superdatorcentrum (NSC), Linköping, Sweden. E.C. and D.C. thank the NSC for a generous allotment of computer time.

Supporting Information Available: Z-Matrixes of compounds **1**, **5**, **6**, and **7** including various conformations and the corresponding transition states. This material is available free of charge via the Internet at http://pubs.acs.org.

References and Notes

(1) Roubi, M. A. *Chem. Eng*. **1995**, *44*, 37.
(2) Japar, S. M.; Wallington, T. J.; Richert, J. F. O.; Ball, J. C. *Int. J. Chem Kinet*. **1990**, *22*, 1257.
(3) Jenkin, M. E.; Hayman, G. D.; Wallington, T. J.; Hurley, M. D.; Ball, J. C.; Nielsen, O. J.; Elllerman, T. *J. Phys Chem*. **1993**, *97*, 11712.
(4) Wallington, T. J.; Hurley, M. D.; Ball, J. C.; Jenkin, M. E. *Chem. Phys. Lett*. **1993**, *211*, 41.
(5) Langer, S.; Ljungstrom, E.; Elllerman, T.; Nielsen, O. J.; Sehested, J. *Chem. Phys. Lett*. **1995**, *240*, 53.
(6) Sehested, J.; Mogelberg, T.; Wallington, T. J.; Kaiser, E. W.; Nielsen, O. J. *J. Phys. Chem*. **1996**, *100*, 17218.
(7) Sehested, J.; Sehested, K.; Platz, J.; Egsgaard, H.; Nielsen, O. J. *Int. J. Chem. Kinet*. **1997**, *29*, 627.
(8) LeFevre, H. F.; Meagher, J. F.; Timmons, R. B. *Int. J. Chem. Kinet*. **1972**, *4*, 103.
(9) Schalley, Ch. A.; Harvey, J. N.; Schröder, D.; Schwarz, H. *J. Phys. Chem. A* **1998**, *102*, 1021.
(10) Lugez, C.; Schriver, A.; Levant, R.; Schriver-Mazzuoli, L. *Chem. Phys.* **1994**, *181*, 129.
(11) Allan, A.; McKean, D. C.; Perchard, J. P.; Josien, M. L. *Spectrochim. Acta, Part A* **1970**, *27a*, 1409.
(12) (a) Turnipseed, A. A.; Vaghjiani, G. L.; Gierczak, T.; Thomson, J. E.; Ravishankara, A. R. *J. Chem. Phys.* **1991**, *95*, 3244. (b) Sedlacek, A. J.; Wight, Ch. A. *J. Chem. Phys.* **1989**, *93*, 509.
(13) Fournier, J.; Deson, J.; Vermeil, C.; Pimentel, G. C. *J. Chem. Phys.* **1979**, *70*, 5726.
(14) Ryan, E. T.; Weitz, E. *Chem. Phys*. **1994**, *189*, 293.
(15) Benderskii, A. V.; Wight, Ch. A. *Chem. Phys*. **1994**, *189*, 307.
(16) Engdahl, A. *Chem. Phys.* **1993**, *178*, 305.
(17) Engdahl, A.; Nelander, B. *J. Chem. Soc., Faraday Trans.* ***1992***, *88*, 177.
(18) Christe, K. O. *Spectrochim. Acta, Part A.* **1971**, *27*, 463.
(19) Glushonok, G. K.; Kovalenko, N. I.; Petryaev, E. P. *Russ. J. Phys. Chem.* **1983**, *57*, 378.
(20) Schuchmann, H.-P.; von Sonntag, C. *J. Photochem.* **1981**, *16*, 289.
(21) Gilbert, B. C.; Holmes, R. G. G.; Laue, H. A. H.; Norman, R. O. C. *J. Chem. Soc., Perkin Trans. 2* **1976**, 1047.
(22) Gilbert, B. C.; Holmes, R. G. G.; Norman, R. O. C. *J. Chem. Res. (S)* **1977**, 1.
(23) Berednikov, V. M.; Bazahin, N. M.; Fedorov, V. K.; Polyakov, O. V. *Kinet. Catal. (Engl. Transl.)* **1972**, *13*, 986.
(24) Wang, W.-F.; Schuchmann, M. N.; Bachler, V.; Schuchmann, H.-P.; von Sonntag, C. *J. Phys. Chem.* **1996**, *100*, 15843.
(25) Jeffrey, G. A.; Pople, J. A.; Radom, L. *Carbohydr. Res.* **1974**, *38*, 81.
(26) Kirby, A. J. *The Anomeric Effect and Related Stereoelectronic Effects at Oxygen*; Springer-Verlag: New York, 1983.
(27) Cremer, D. *J. Chem. Phys.* **1978**, *69*, 4456.
(28) (a) Liedtke, M.; Saleck, A. H.; Yamada, K. M. T.; Winnewisser, G.; Cremer, D.; Kraka, E.; Dolgner, A.; Hahn, J.; Dobos, S. *J. Phys. Chem.* **1993**, *97*, 11204. (b) Landin, J.; Pascher, I.; Cremer, D. *J. Phys. Chem.* **1995**, *99*, 4471.
(29) (a) Cremer, D.; Binkley, J. S.; Pople, J. A.; Hehre, W. J. *J. Am. Chem. Soc*. **1974**, *96*, 6900. (b) Munoz-Caro, C.; Nino, A.; Senent, M. L. *Chem. Phys. Lett*. **1997**, *273*, 135. For a recent review, see: (c) Goodman, L.; Pophristic, V. In *Encyclopedia of Computational Chemistry*; Schleyer, P. v. R., Allinger, N. L., Clark, T., Gasteiger, J., Kollman, P. A., Schaefer, H. F., III, Schreiner, P. R., Eds.; John Wiley: Chichester, U.K., 1998; Vol. 4, p 2525.
(30) (a) Curtiss, L. A.; Raghavachari, K.; Trucks G. W.; Pople, J. A. *J. Chem. Phys.* **1991**, *94*, 7221. (b) Pople, J. A.; Head-Gordon, M.; Fox, D. J.; Raghavachari, K.; Curtiss, L. A. *J. Chem. Phys*. **1989**, *90*, 5622.
(31) (a) Chase, M. W.; Curnutt, J. L.; Downey, J. R.; MacDonald, R. A.; Syverud, A. N.; Valenzuela, E. A. JANAF Thermochemical Tables. *J. Phys. Chem. Ref. Data* **1982**, *11*, 695. (b) Chase, M. W.; Davies, C. A.; Downey, J. R.; Frurip, D. J.; McDonald, R. A.; Syverud, A. N. JANAF

Thermochemical Tables, 3rd ed. *J. Phys. Chem. Ref. Data* **1985**, *14* (Suppl. 1), 1. (c) Pedley, J. B.; Naylor, R. D.; Kirby, S. P. *Thermochemical Data of Organic Compounds*, 2nd ed.; Chapman and Hall: New York, 1986.

(32) (a) Golden, D. M.; Benson, S. W. *Chem. Rev.* **1969**, *69*, 125. (b) Cruickshank, F. R.; Benson, S. W. *Int. J. Chem. Kinet.* **1969**, *1*, 381. (c) Holmes, J. L.; Lossing, F. P. *Int. J. Mass. Spectrom. Ion Processes* **1984**, *58*, 113.

(33) Good, D. A.; Francisco, J. S. *Chem. Phys. Lett.* **1997**, *266*, 512.

(34) Most of the available information concerns metal atom, closed-shell interactions. See, e.g.: (a) Curtiss, L. A.; Kraka, E.; Gauss, J.; Cremer, D. *J. Phys. Chem.* **1987**, *91*, 1080. (b) Erickson, L. A. In *Density-Functional Methods in Chemistry and Material Science*. Springborg, M., Ed.; Wiley: New York, 1997; p 125.

(35) (a) Houk, K. N.; Rodan, N. G.; Mareda, J. *J. Am. Chem. Soc.* **1984**, *106*, 4291. (b) Houk, K. N.; Rodan, N. G. *J. Am. Chem. Soc.* **1984**, *106*, 4293. (c) Blake, J. F.; Wierschke, S. G.; Jorgensen, W. L. *J. Am. Chem. Soc.* **1989**, *111*, 1919.

(36) Johnson, B. G.; Gonzales, C. A.; Gill, P. M. W.; Pople, J. A. *Chem. Phys. Lett.* **1994**, *221*, 100.

(37) (a) Baker, J.; Muir, M.; Andzelm, J. *J. Chem. Phys.* **1994**, *102*, 2063. (b) Baker, J.; Andzelm, J.; Muir, M.; Taylor, P. R. *Chem. Phys. Lett.* **1995**, *237*, 53.

(38) Johnson, B. G. In *Theoretical and Computational Chemistry: Density Functional Calculations*; Politzer, P., Seminario, J. M., Eds.; Elsevier: Amsterdam, in press.

(39) Perdew, J. P.; Zunger, A. *Phys. Rev. B* **1981**, *23*, 5048.

(40) (a) Pederson, M. R.; Lin, C. C. *J. Chem. Phys.* **1988**, *88*, 1807. (b) Fois, E. S.; Penman, J. I.; Madden, P. A. *J. Chem. Phys.* **1993**, *98*, 6352.

(41) Becke, A. D. *J. Chem. Phys.* **1993**, *98*, 5648.

(42) Adamo, C.; Barone, W. *Chem. Phys. Lett.* **1997**, *247*, 242.

(43) Nova, J. J.; Sosa, C. *J. Phys. Chem.* **1995**, *99*, 1141.

(44) (a) Kristyan, S.; Pulay, P. *Chem. Phys. Lett.* **1994**, *229*, 175. (b) Hobza, P.; Sponer, J.; Reschel, T. *J. Comput. Chem.* **1995**, *16*, 1315. (c) Ruiz, E.; Salahub, D. R.; Vela, A. *J. Am. Chem. Soc.* **1995**, *117*, 1141.

(45) (a) Konkoli, Z.; Cremer, D. *Int. J. Quantum Chem.* **1998**, *67*, 1. (b) Konkoli, Z.; Larsson, J. A.; Cremer, D. *Int. J. Quantum Chem.* **1998**, *67*, 11. (c) Konkoli, Z.; Cremer, D. *Int. J. Quantum Chem.* **1998**, *67*, 29. (d) Konkoli, Z.; Larsson, J. A.; Cremer, D. *Int. J. Quantum Chem.* **1998**, *67*, 41.

(46) Cremer, D.; Larsson, J. A.; Kraka, E. In *Theoretical and Computational Chemistry*: *Theoretical Organic Chemistry*; Parkanyi, C., Ed.; Elsevier: Amsterdam, 1998; Vol. 5, p 259.

(47) Larsson, J. A.; Cremer, D. To be published.

(48) Wigner, E. P. *Z. Phys. Chem. B* **1932**, *19*, 203. (b) Bell, R. P. *The Tunnel Effect in Chemistry*; Chapman: London, 1980.

(49) Kraka, E.; Gauss, J.; Cremer, D. *J. Chem. Phys.* **1993**, *99*, 5306.

(50) Del Bene, J. E. In *Encyclopedia of Computational Chemistry*; Schleyer, P. v. R., Allinger, N. L., Clark, T., Gasteiger, J., Kollman, P. A., Schaefer, H. F., III, Schreiner, P. R., Eds.; John Wiley: Chichester, U.K., 1998; Vol. 2, p 1263.

(51) Benson, S. W. *Thermochemical Kinetics*; John Wiley: New York, 1968.

(52) Bernardi, F.; Epiotis, N. D.; Cherry, W.; Schlegel, H. B.; Whangbo, M.-H.; Wolfe, S. *J. Am. Chem. Soc.* **1976**, *98*, 469.

(53) Gardiner, W. C. *Combustion Chemistry*; Springer: New York, 1984.

(54) 6-31G(d): Hariharan, P. C.; Pople, J. A. *Chem. Phys. Lett.* **1972**, *66*, 217. 6-311G(d): Krishnan, R.; Frisch, M. J.; Pople, J. A. *Chem. Phys.* **1980**, *72*, 4244.

(55) For a recent review, see: Cremer, D. In *Encyclopedia of Computational Chemistry;* Schleyer, P. v. R., Allinger, N. L., Clark, T., Gasteiger, J., Kollman, P. A., Schaefer, H. F., III, Schreiner, P. R., Eds.; John Wiley: Chichester, U.K., 1998; Vol. 3, p 1706.

(56) For a recent review, see: Gauss, J. In *Encyclopedia of Computational Chemistry*; Schleyer, P. v. R., Allinger, N. L., Clark, T., Gasteiger, J., Kollman, P. A., Schaefer, H. F., III, Schreiner, P. R., Eds.; John Wiley: Chichester, U.K., 1998; Vol. 1, p 615.

(57) Miller, W. H.; Handy, N. C.; Adams, J. E. *J. Chem. Phys.* **1980**, *72*, 99.

(58) Boys, F.; Bernardi, F. *Mol. Phys.* **1970**, *19*, 553.

(59) Kraka, E.; Gräfenstein, J.; Gauss, J.; He, Z.; Konkoli, Z.; Olsson, L.; Reichel, F.; Cremer, D. *COLOGNE98*; Göteborg, 1998.

(60) Stanton, J. F.; Gauss, J.; Watts, J. D.; Lauderdale, W. J.; Bartlett, R. J. *ACES II*; *Quantum Theory Project*; University of Florida, 1992.

(61) Frisch, M. J.; Trucks, G. W.; Schlegel, H. B.; Gill, P. M. W.; Johnson, B. G.; Robb, M. A.; Cheeseman, J. R.; Keith, T.; Petersson, G. A.; Montgomery, J. A.; Raghavachari, K.; Al-Laham, M. A.; Zakrzewski, V. G.; Ortiz, J. V.; Foresman, J. B.; Peng, C. Y.; Ayala, P. Y.; Chen, W.; Wong, M. W.; Andres, J. L.; Replogle, E. S.; Gomperts, R.; Martin, R. L.; Fox, D. J.; Binkley, J. S.; Defrees, D. J.; Baker, J.; Stewart, J. P.; Head-Gordon, M.; Gonzalez, C.; Pople, J. A. *Gaussian 94*, revision B.3; Gaussian, Inc.: Pittsburgh, PA, 1995.

(62) Frisch, M. J.; Trucks, G. W.; Schlegel, H. B.; Scuseria, G. E.; Robb, M. A.; Cheeseman, J. R.; Zakrzewski, V. G.; Montgomery, J. A., Jr.; Stratmann, R. E.; Burant, J. C.; Dapprich, S.; Millam, J. M.; Daniels, A. D.; Kudin, K. N.; Strain, M. C.; Farkas, O.; Tomasi, J.; Barone, V.; Cossi, M.; Cammi, R.; Mennucci, B.; Pomelli, C.; Adamo, C.; Clifford, S.; Ochterski, J.; Petersson, G. A.; Ayala, P. Y.; Cui, Q.; Morokuma, K.; Malick, D. K.; Rabuck, A. D.; Raghavachari, K.; Foresman, J. B.; Cioslowski, J.; Ortiz, J. V.; Stefanov, B. B.; Liu, G.; Liashenko, A.; Piskorz, P.; Komaromi, I.; Gomperts, R.; Martin, R. L.; Fox, D. J.; Keith, T.; Al-Laham, M. A.; Peng, C. Y.; Nanayakkara, A.; Gonzalez, C.; Challacombe, M.; Gill, P. M. W.; Johnson, B.; Chen, W.; Wong, M. W.; Andres, J. L.; Gonzalez, C.; Head-Gordon, M.; Replogle, E. S.; Pople, J. A. *Gaussian 98*, revision A.5; Gaussian, Inc.: Pittsburgh, PA, 1998.

(63) Kanazawa, Y.; Nukada, K. *Bull. Chem. Soc. Jpn.*. **1962**, *35*, 612.

(64) Blukis, U.; Kasai, P. H.; Myers, R. J. *J. Chem. Phys.* **1963**, *38*, 2753.

(65) Träubel, M. Zur Thermo- und Photochemie von 1,2,3- und 1,2,4-trioxolanen, Ph.D. Thesis, TU Braunschweig, 1994.